# Abstract

*Background and Purpose:*

Paediatric posterior fossa tumours often present with hydrocephalus and post-operatively up to 25% develop cerebellar mutism syndrome (CMS). Arterial spin labelling (ASL) MRI is a non-invasive means of quantifying cerebral blood flow (CBF) and bolus arrival time (BAT). The aim of this study was to investigate how changes in perfusion metrics in children with posterior fossa tumours were modulated by CMS and hydrocephalus requiring pre-resection CSF diversion.

*Materials and Methods:*

44 patients were prospectively scanned at three timepoints (pre-operatively, post-operatively and at 3 months follow-up) with single- and multi-inflow time ASL sequences. Regional analyses of CBF and BAT were conducted using co-registered anatomical parcellations. ANOVA and multivariable linear mixed-effects modelling analysis approaches were used. Registered at clinicaltrials.gov (NCT03471026).

*Results:*

CBF increased after tumour resection, and at follow-up scanning ($p=0.045$). BAT decreased after tumour resection, and at follow-up scanning ($p=0.018$). BAT was prolonged ($p=0.058$) following midline, as compared to cerebellar hemispheric surgical approaches to posterior fossa tumours. Multivariable linear mixed-effects modelling showed regional perfusion changes were more pronounced in the six children who presented with symptomatic obstructive hydrocephalus requiring pre-resection CSF diversion, with hydrocephalus lowering baseline CBF by 20.5±6.27 ml/100g/min (mean±S.E.). Children diagnosed with cerebellar mutism syndrome (8/44, 18.2%) had significantly higher CBF at follow-up imaging than those without ($p=0.040$), but no differences in pre- or post-operative perfusion parameters were seen.

*Conclusion:*

Multi-TI ASL shows promise as a non-invasive tool to evaluate cerebral perfusion in the setting of paediatric obstructive hydrocephalus, and demonstrates increased CBF following CMS resolution.

## Keywords

Brain tumour; Cerebellar mutism syndrome; Hydrocephalus, MultiTI ASL; Paediatric

## Abbreviations

ASL, arterial spin labelling; BAT, bolus arrival time; BuxCBF, Buxton-modelled CBF from multi-TI ASL data; CMS, cerebellar mutism syndrome; EVD, external ventricular drain; GA, general anaesthetic; ICP, intracranial pressure; PLD, post-labelling delay.

# 1. Introduction

CBF is a physiological parameter with a well-established relationship to intracranial pressure (ICP) and systemic arterial blood pressure[1–3]. Changes in CBF follow open craniotomy in adult patients[4], but less is known about the effect of neurosurgery on CBF in children[5]. Brain tumours commonly occur in the posterior fossa in children, who often present with symptoms of raised ICP due to obstruction of CSF flow[6]. Obstructive hydrocephalus can be severe enough to warrant emergency CSF diversion as a life-saving procedure prior to tumour resection. There are few reports of alterations in perfusion metrics in children with hydrocephalus[5,7,8]. Following tumour resection, up to a quarter of patients develop cerebellar mutism syndrome (CMS)[9], characterised by a delayed onset of mutism and emotional lability[10] which tend to resolve over a period of weeks to months. Damage to the superior cerebellar peduncles is thought to disturb reciprocal cerebro-cerebellar pathways giving rise to the striking symptomatology of the condition. Frontal perfusion deficits in CMS patients have previously been shown using SPECT imaging[11,12], DSC MRI[13], and more recently using arterial spin labelling MRI (ASL)[14,15].

ASL quantifies brain perfusion in physiologically relevant units by subtracting an image with radiofrequency-labelled blood, from a control image, at a suitable post-labelling delay (PLD, also known as single inflow-time or single-TI data). By acquiring data at multiple inflow times (multi-TI), it is possible to extract further parameters, such as the bolus arrival time (BAT) of labelled blood. BAT varies regionally, making single-PLD acquisitions susceptible to underestimation of CBF due to incomplete delivery of the bolus of labelled blood at the chosen inflow time. The advantage of multi-TI ASL is that this is accounted for by imaging at serially increasing inflow times.

The aim of this study was to characterise perfusion metrics of CBF and BAT of labelled blood, using single- and multi-TI ASL, in children with posterior fossa tumours. We also aimed to investigate how changes in perfusion metrics were modulated by peri-operative surgical and clinical features of CMS, and hydrocephalus requiring pre-resection CSF

diversion. We hypothesised that children with CMS would have reduced CBF post-operatively, and that hydrocephalus would cause reductions in pre-operative CBF and prolong pre-operative BAT.

# 2. Methods

## 2.1 Patients

Children referred to our institution with posterior fossa tumours underwent MRI scanning prior to tumour resection, within 72h of tumour resection, and at 3-month follow up. Scans were carried out under general anaesthetic (GA) in younger children to avoid movement artefacts; otherwise, all scanning was in unsedated patients. Sedation requirements were assessed by experienced paediatric neuroradiographers prior to scanning and were primarily determined by patient age. Only one patient required GA at a follow-up scan appointment, having previously tolerated unsedated scanning.

Children presenting with symptomatic hydrocephalus (signs of raised ICP, such as headache, vomiting, or deteriorating conscious level) were treated with urgent CSF diversion in the form of an external ventricular drain (EVD) prior to tumour resection. Those who did not undergo pre-resection EVD were temporised with glucocorticoid administration until tumour resection. Operative notes were contemporaneously reviewed and intradural surgical approach to the tumour was categorised into midline, hemispheric, and miscellaneous groups. Post-operative CMS status was determined by prospective clinical evaluation by attending neurosurgical and multidisciplinary staff. The diagnosis was primarily based on the presence of mutism or reduced speech output in the early post-operative phase. Patients were followed up at 2-months post-operatively to assess for ongoing symptoms of CMS. Ethical approval was granted by the NHS HRA (18/LO/0501), and the study was registered at clinicaltrials.gov (NCT03471026).

## 2.2 MR acquisition

Imaging was performed on a 3T MRI scanner (Prisma, Siemens Healthcare, Erlangen, Germany) using a 20-channel head receive coil. The scanning protocol comprised structural imaging (including T1 MPRAGE), multi-shell diffusion imaging (dMRI), and ASL MRI. Imaging at the pre-operative timepoint was acquired prior to CSF diversion.

Single-PLD ASL was performed using a prototype pseudo-continuous labelling sequence (pCASL; Siemens Healthcare, Erlangen, Germany), with background suppression, and a 3D gradient-and-spin-echo readout. Imaging parameters were set according to international consensus recommendations[16], with a labelling duration of 1800ms, a 1500ms post-labelling delay, and 10 repetitions. The field of view (FOV) was 220mm, with a 64 x 62 matrix, reconstructed to 1.7 x 1.7 $mm^2$ in-plane spatial resolution (interpolation factor 2). Additional sequence parameters were: 24 partitions; turbo factor=12, EPI factor=31, segments=2 (with parallel imaging, GRAPPA=2), slice thickness = 4.0 mm; TR = 4620ms; TE = 21.8ms. A proton-density weighted (M0) image was also acquired, with identical readout as the ASL acquisition but with the labelling RF pulses removed, for CBF quantification.

Multi-TI pulsed ASL (PASL) data were comprised of acquisitions at 10 inflow times (TIs) ranging from 350 to 2600ms in 250ms steps, with a single acquisition per TI. The TR was 3300ms; all other readout parameters were as above.

## 2.3 Image processing

Cortical parcellation and subcortical segmentation were performed on volumetric T1-weighted images using Freesurfer[17], and these were registered into patients' diffusion space using *Niftyreg*[18]. Repetitions of raw ASL images were checked for motion artefacts prior to averaging. Preprocessing of all ASL data was performed in Matlab (R2017b, Mathworks Inc., Natick, MA). Single-PLD data was pre-processed using the method of Alsop *et al*.[16] to calculate voxel-wise CBF (ml/100g/min). The kinetic model described by Buxton *et al.*[19] was used on noise-masked

multi-TI ASL data to calculate voxel-wise maps of BAT (seconds) and CBF (ml/100g/min; referred to in section 3 as BuxCBF to avoid confusion with CBF from single-PLD data). Details of the model fitting procedure are described elsewhere[20]. Each patient's ASL parameter maps were registered into patients' diffusion space using FSL Flirt[21] (FSL v 5.0.10, Oxford, UK). Diffusion space was chosen as a symmetrical registration space as its resolution was midway between that of ASL and structural images. Timepoint- and subject-specific median perfusion parameters were then extracted for regions corresponding to frontal, parietal, occipital, temporal and motor (precentral, paracentral and caudal middle frontal gyri) cortex, thalamus and cerebellum.

## 2.4 Statistical Analysis

Statistical analysis was performed in R[22] (v3.6.1). Continuous data were tested for differences in means using a two-tailed Student's *t*-test after assessing assumptions of normality using the Shapiro-Wilk test. Non-normally distributed data were tested using the Wilcoxon rank-sum test. A pre-specified $\alpha$ of 0.05 was chosen. A one-way repeated measures ANOVA was conducted to examine the effect of scanning timepoint on perfusion metrics. Subsequent group comparisons using pairwise t-tests were corrected for multiple comparisons using the false discovery rate.

A multivariable linear mixed-effect modelling analysis was performed in which subject ID was taken as a random effect, and fixed effects included scanning timepoint, brain region, age, sedation status, hydrocephalus, and CMS. The Akaike Information Criterion (AIC), and marginal / conditional $R^2$ values[23] were used to assess model performance. Model performance was taken to be improved with a lower AIC, and/or an increase in $R^2$. Likelihood ratio (LR) ANOVA tests were used to assess the effects of additive model terms.

# 3. Results

44 patients were prospectively recruited to the study, with a mean age of 6.69 years (S.D. 3.68, range 1.04-14.6); 23 were female. The most

common tumour histology encountered at operation was pilocytic astrocytoma (PA; 22), followed by medulloblastoma (14), ependymoma (2), diffuse midline glioma (DMG; 2), and atypical teratoid/rhabdoid tumour (ATRT), ganglioglioma, haemangioblastoma, and high grade glioma (1 each). Six patients (13.6%) underwent pre-operative CSF diversion due to symptomatic obstructive hydrocephalus. The majority of patients (23/44, 52.3%) underwent midline intradural surgical approaches to the tumour. Eleven patients (25.0%) underwent lateral transcerebellar hemispheric approaches, and the remaining 10 patients (22.7%) had heterogeneous surgical approaches to their tumour including biopsy only, cerebellopontine angle or direct access to large tumours presenting to the parenchymal surface. Eight patients (18.2%) were diagnosed with CMS in the post-operative period. The cardinal symptom of mutism was improved in five of these patients at follow-up. Eleven patients in the cohort (25.0%, all medulloblastoma) underwent adjuvant photon radiotherapy.

## 3.1 Change in gross perfusion metrics

Mean CBF in the cerebral cortex increased across the three timepoints (pre-op mean±S.D.: 39.6±13.3ml/100g/min; post-op: 45.5±13.3ml/100g/min; follow-up: 51.5±12.6ml/100g/min; Figure 1A). Repeated measures ANOVA revealed statistically significant differences between the three timepoints (p=0.045), although *post-hoc* tests did not survive multiple comparison correction. Mean regional BAT decreased over time (pre-op: 0.982±0.069s; post-op: 0.884±0.083s; follow-up: 0.747±0.217s; Figure 1B). Repeated measures ANOVA revealed statistically significant differences between the three timepoints (p=0.018), and *post-hoc* tests confirmed a significant difference between the pre-operative and follow-up timepoints (p=0.034). Single-PLD CBF results were echoed by similar trends in mean BuxCBF, although these did not reach statistical significance (pre-op: 90.2±36.9ml/100g/min; post-op 113±33.3ml/100g/min; follow-up 112±51.7ml/100g/min; *p*=0.129; Figure 1C). Examples of single-PLD and multi-TI ASL data from a single representative patient are shown in Figure 2.

Table 1 shows differences in perfusion metrics of the cerebral cortex at the post-operative timepoint, depending on the surgical approach used. There was no significant difference in post-operative CBF between midline and lateral surgical approaches (p=0.212, 0.209 respectively), and no difference in mean age between the two groups (p=0.527). Cortical BAT appeared to be prolonged in children who had undergone a midline approach to the tumour, although this did not reach statistical significance (p=0.058).

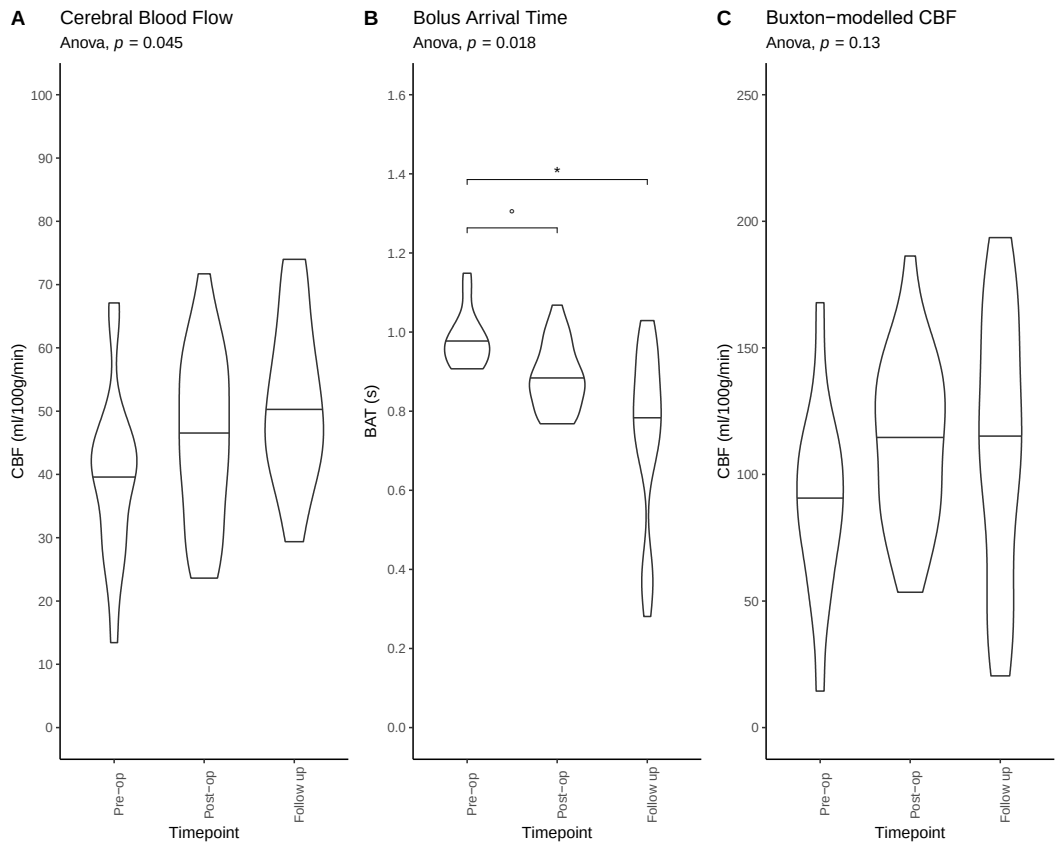


**Figure 1**. Violin plots showing change in perfusion metrics across timepoints for all patients' brain regions. Horizontal line within plot indicates median. Darker datapoints indicate patients with CMS. **A**, cerebral blood flow derived from single-PLD ASL. **B**, bolus arrival time derived from multi-TI ASL. **C**, cerebral blood flow derived from multi-TI ASL. Horizontal significance bars show false discovery rate adjusted *p*-values from *t*-test pairwise comparisons °, p<0.1; *, p<0.05.

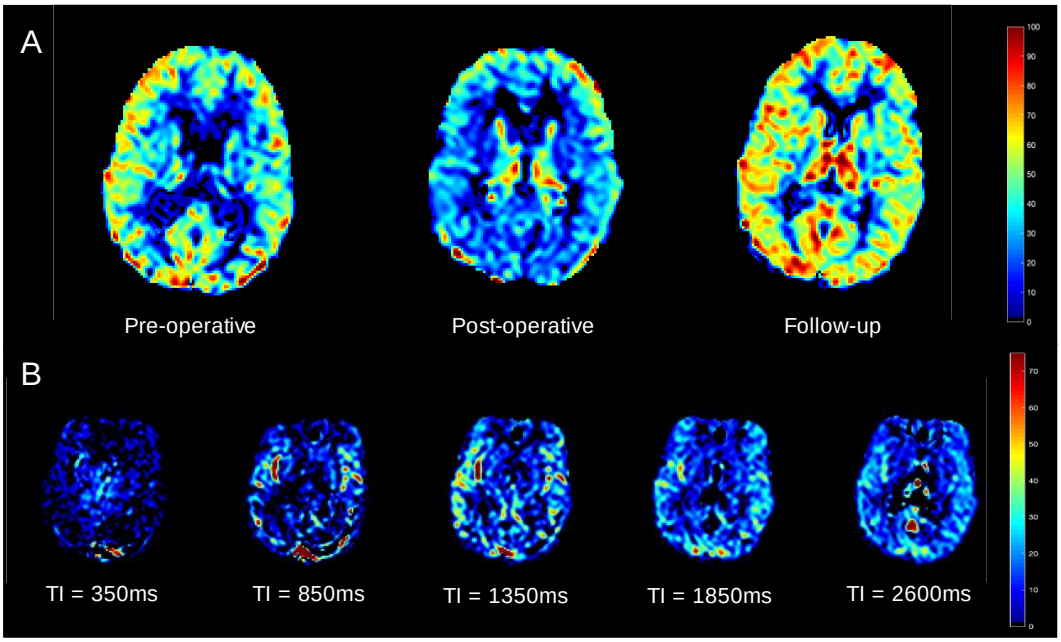


**Figure 2**. Example ASL maps of a patient with a posterior fossa pilocytic astrocytoma on a mid-thalamic axial slice. **A**, single-PLD CBF maps at pre-operative, post-operative and follow-up timepoints. Colour bar indicates ml/100g/min. **B**, raw multi-TI ASL data showing difference in magnetisation (d*M*) between control and label scans at selected sequentially increasing inflow times at a follow-up scan. Colour bar indicates arbitrary units of *dM*.

## 3.2 Perfusion and Hydrocephalus

There was no significant difference in age between those with and without symptomatic obstructive hydrocephalus requiring pre-resection CSF diversion (p=0.277). In patients with hydrocephalus, pre-operative mean cortical CBF was lower than in those who had not required CSF diversion (mean±S.D., 22.2±8.95 vs 43.1±11.2ml/100g/min, p=0.032). These effects were observed for all brain regions studied (Figure 3A), and differences in all regions reached a level of statistical significance apart from frontal and motor cortices. Post-operatively, mean cortical CBF returned to normal levels, with no statistically significant difference in cortical CBF between those who underwent CSF diversion and those who did not (48.3±10.7 vs 45.0±13.8ml/100g/min, p=0.562). At follow-up imaging, mean cortical CBF was 57.5±16.5ml/100g/min in the hydrocephalus group compared to 50.3±11.8ml/100g/min in those without hydrocephalus (p=0.396). These results were echoed by the findings from cortical BuxCBF, although these

did not reach statistical significance at any timepoint (all p=0.183). Furthermore, a regional analysis did not reveal any statistically significant differences in BuxCBF between groups, other than in the thalamus at the pre-operative timepoint (p=0.014).

There was a statistically significant prolongation of bolus arrival time to the cerebral cortex pre-operatively in children with symptomatic hydrocephalus (1.09±0.07 vs 0.954±0.037s, p=0.048). Figure 3B shows that this was more striking in some supratentorial cortical regions, especially frontal, motor and occipital parcels. Post-operatively and at follow-up, there were no significant differences in mean cortical BAT dependent on pre-resection hydrocephalus treatment (p=0.153, 0.558 respectively).

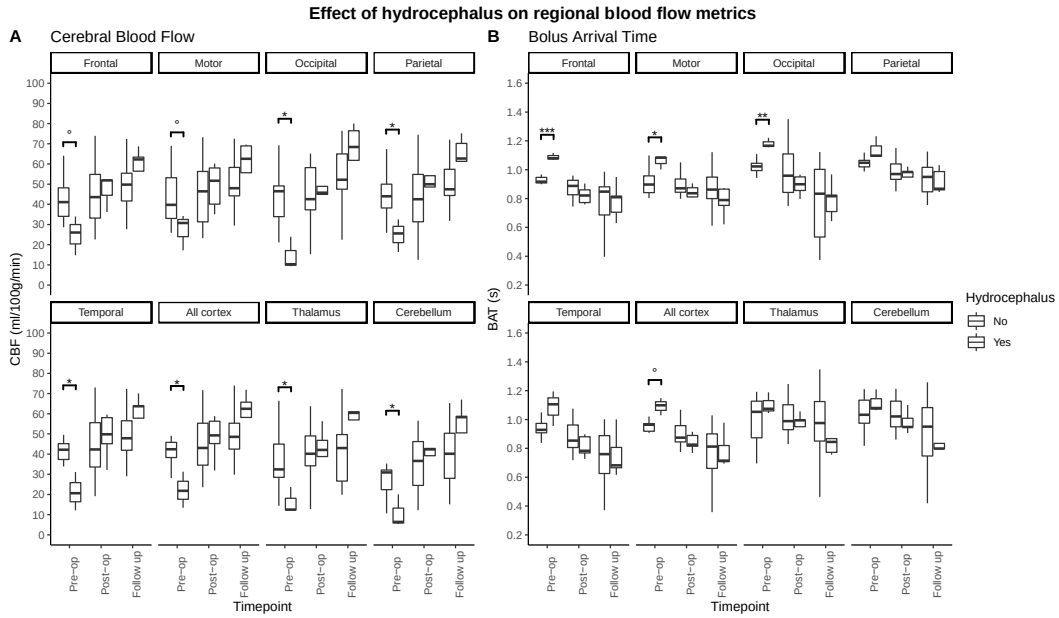


**Figure 3**. Boxplots depicting perfusion metrics stratified by brain regions in patients with and without symptomatic hydrocephalus. **A**, cerebral blood flow derived from single-PLD ASL. **B**, bolus arrival time derived from multi-TI ASL. False discovery rate-adjusted *p*-values: °, p<0.1; *, p<0.05; **, p<0.01; ***, p<0.001.

## 3.3 Perfusion and CMS

There was a significant difference in age between children diagnosed with CMS post-operatively and those without (mean±S.D. 4.00±1.90 vs 7.20±3.72 years, p=0.002). Pre-operative (42.2±2.88 vs 39.3±14.1ml/100g/min, p=0.488) and post-operative (48.6±10.9 vs 44.8 ±

13.9ml/100g/min, p=0.484) mean cortical CBF was similar between children with CMS and those without. There was a significantly higher mean CBF at the follow-up timepoint in the CMS group (57.5± 6.08 vs 49.7±13.6ml/100g/min, p=0.040). There were no significant differences in BAT or BuxCBF at any timepoint, and no significant differences in any perfusion metrics on a regional analysis.

## 3.4 Linear mixed-effects modelling

Multivariable linear mixed-effects models were used to explore the effect of hydrocephalus and CMS on CBF in the cohort. Models were fit on a three-region sample of CBF values: the mean across the whole cortex, thalamus and cerebellum. This process began with the fitting of a baseline model (mod_baseline) which did not include the effects of interest, in order to estimate the effects of timepoint, age and brain region on CBF. Model terms and their fixed-effect coefficients are shown in Table 2, along with comparisons of model characteristics.

The addition of hydrocephalus with an interaction term for timepoint (mod_hcp) reduced the AIC and increased $R^2$ values. LR testing of mod_hcp2 and mod_baseline indicated a significant effect of hydrocephalus and its interaction with timepoint on the model ($p<0.0001$). The full model (mod_hcpcms) included terms for CMS and HCP and their interactions with timepoint. LR testing between the two best-performing models, mod_hcp and mod_hcpcms, showed a statistically significant difference between the two in favour of the full model (p=0.03), which also had the lowest AIC and higher $R^2$ values.

# 4. Discussion

In this prospective study of children with posterior fossa tumours, mean cortical CBF increased after tumour resection and at follow-up imaging. For the first time we show reductions in BAT of labelled blood to the cerebral cortex after tumour resection. Children presenting with symptomatic obstructive hydrocephalus requiring pre-resection CSF diversion had significantly reduced pre-operative CBF and prolonged BAT.

A regional analysis according to standardised brain parcellations revealed that CBF was significantly lower pre-operatively in many cortical regions in patients with hydrocephalus; and that BAT was significantly prolonged in the frontal, motor and occipital cortex of patients with hydrocephalus. There was a significantly higher CBF at follow-up in children who developed CMS. A multivariable linear mixed-effect modelling approach confirmed that both hydrocephalus and CMS had a significant effect on CBF by timepoint. In fact, these two factors emerged as more significant features of determining post-operative CBF in the final model than timepoint alone.

Our results indicate weak evidence of prolonged BAT after midline approaches to posterior fossa tumours, which entail more extensive dissection of neural parenchyma, greater exposure of CSF spaces, and increased handling and manipulation of large infratentorial arteries, such as the posterior inferior cerebellar artery (PICA). It is possible that vasospasm could have led to prolonged BAT following midline approaches. This has been described following posterior fossa tumour resection in children[24,25], and even described as a cause of CMS in an adolescent[26].

## 4.1 Perfusion metrics and hydrocephalus

70-90% of children with posterior fossa tumours present with hydrocephalus[27]. However, the relationship between ventricular size, compliance and pressure is complex, and ventricular size can be equivocal with regard to underlying CSF mechanics[28]. In this series, the need for pre-resection CSF diversion was judged clinically, by experienced paediatric neurosurgeons, based on features of raised ICP. It is to be expected that resection of a posterior fossa tumour alone will increase CBF due to the removal of an obstructing mass[5], however we demonstrate that in patients with symptomatic hydrocephalus prior to tumour resection, mean cortical CBF was lower and BAT was higher, with statistically significant differences in these parameters between groups.

The first study to evaluate the role of ASL imaging in hydrocephalus compared 19 patients with hydrocephalus secondary to posterior fossa tumours, with 16 healthy controls[7]. The former group were found to have significantly lower CBF at baseline. CBF was significantly increased in this group after “alleviation of hydrocephalus”, i.e. tumour resection (with additional CSF diversion in 6 patients). The present study replicates these findings, and by adding a temporal dimension in the form of multi-TI ASL, is the first demonstration that reduction of CBF in symptomatic obstructive hydrocephalus occurs in conjunction with a prolonged arterial transit time. A regional analysis of perfusion metrics showed that CBF was lower in the hydrocephalus group for all brain regions other than frontal and motor cortices. This is likely to be due to the raised ICP related to hydrocephalus causing reduced cerebral perfusion pressure. However, as the ICP was not directly measured in this study we cannot provide any mechanistic evidence for this.

Changes in BuxCBF in the hydrocephalus group were correspondent in direction, although only comparison of the pre-operative thalamic BuxCBF reached a level of statistical significance. BuxCBF values are inevitably higher than single-PLD CBF values as they capture blood flow in large arteries at earlier inflow times. The concordance between these two metrics provides reassurance that the single-PLD CBF changes were not due to incomplete delivery of the labelled bolus at the post-labelling delay of 1.5s.

The results of the linear multivariable mixed-effects modelling confirmed the effects of hydrocephalus on CBF seen by statistical hypothesis testing of the data. This indicated that hydrocephalus had a significant effect on CBF dependent on timepoint, once age, sedation status, brain region, scanning timepoint and CMS by timepoint were controlled for, reducing CBF by 20.5±6.27 ml/100g/min pre-operatively ($p<0.01$). Following tumour resection, children who had been treated with CSF diversion had significant increases in CBF at post-operative imaging (24.0±5.13 ml/100g/min, $p<0.001$), and at follow-up imaging (27.2±5.18 ml/100g/min, $p<0.001$).

One potential clinical implication of these results, when taken alongside those of Yeom *et al*.[7], is that in the presence of equivocal symptomatology of raised ICP, perfusion metrics from ASL may be of assistance in decisions regarding peri-operative CSF diversion. In order to further investigate this possibility, dedicated studies employing real-time ICP measurements, ventricular volumetry and detailed clinical correlates are needed.

## 4.2 Perfusion metrics and CMS

CMS is a common post-operative complication after posterior fossa tumour resection, occurring in around a quarter of cases[6]. The putative mechanism posits damage to the superior cerebellar peduncle at surgery as a key element, causing a disturbance in cerebello-cerebral circuitry. This in turn is thought to lead to diaschisis causing a loss of function in widespread supratentorial cortical areas, and the corollary hypoperfusion can be quantified with perfusion imaging. Thus, SPECT[11,12] and DSC-MRI[13] studies have shown frontal hypoperfusion in patients with CMS. Similarly, ASL-derived CBF was found to be reduced in the frontal lobes in a patient with CMS, recovering to normal levels after resolution of the syndrome[15]. This was later confirmed in a small cohort study of children with posterior fossa tumours (11 patients with CMS compared to 10 without)[14]. A modest reduction in CBF in the right frontal lobe was observed post-operatively, with significant increases in CBF in both frontal lobes after clinical improvement. A systematic review of 5 studies concluded that cerebral perfusion is reduced in children with CMS post-operatively, although none of the included studies incorporated pre-operative comparison imaging[29].

In this study, we were unable to replicate the findings of a statistically significant difference in post-operative CBF with respect to CMS status. However, we provide confirmatory evidence of increased CBF in children with CMS at the follow-up timepoint – after improvement of CMS symptoms in most – on single-PLD CBF (p=0.0403). The multi-TI ASL

results did not demonstrate any differences in BAT or BuxCBF between groups.

The presence of an unbalanced age distribution between groups may go some way towards explaining the results from statistical hypothesis testing of the data. Age is known to be broadly negatively correlated with CBF in children[20] (confirmed by its significance in the final mixed-effects model with a model coefficient of -1.34), so the CMS group having a much younger mean age may have increased the CBF at all timepoints for this group. Other reasons for the lack of distinction in post-operative CBF include a small sample size in the CMS group which will have hindered comparative statistical testing. Furthermore, the repeated measures data are unbalanced, due to the substantial logistical challenges in obtaining pre-operative scans in many patients.

The linear mixed effects models described above are able to circumvent this drawback to give meaningful insights into the effects of this parameter in the cohort. The full model, which included both hydrocephalus and CMS with their timepoint interactions as terms, confirmed a significant increase in CBF in the CMS group at follow-up, and coefficients for the other timepoints almost reached the threshold for statistical significance. The results presented here indicate that future studies investigating perfusion in CMS must take clinical features such as hydrocephalus and tumour location (and therefore surgical approach) into account.

## 4.3 Limitations

The lack of a clear, objective determination of CMS status is a perennial issue in studies reporting neuroimaging correlates of the syndrome and this criticism applies to this study as much as all others in the field. To mitigate against this, the definition of CMS applied in this study was pragmatic, based on the key criterion of mutism or reduced speech output, applied contemporaneously by an experienced neurosurgical multi-disciplinary team. As the key clinical correlate in this study was speech deficit in CMS, it is not known from the data presented herein whether CBF alterations exist post-operatively in the setting of CMS symptoms

other than speech deficit. The development of a validated scoring system for CMS is essential in order to objectively classify CMS phenotypes and their imaging correlates.

The regional ASL analysis did not take into account laterality as the assumption was made that symmetric vasculature leads to symmetric blood delivery. This assumption is perfectly valid in healthy brains, yet may not hold entirely true in a post-operative cohort, with data acquisition shortly after surgery. For instance, unilateral manipulation of major infratentorial arteries, such as the PICA – a necessary step during midline tumour approach in dissection of the posterior fossa – may conceivably have caused a degree of arterial spasm leading to a variation in CBF by laterality.

The parcellation of the brain into regions of cortical lobes in this analysis was a pragmatic one, as we are ultimately interested in behavioural effects of CBF changes in this cohort. However, we recognise that cerebral lobes are functional, not vascular units, and to interrogate perfusion on a truly vascular basis would require territorial ASL[30], which is technically challenging, even more so in unwell peri-operative paediatric patients. The multi-TI ASL acquisition was a research sequence which is not widely available and this limits the generalisability of the results.

With regard to the insights shown on CBF in symptomatic hydrocephalus in the setting of paediatric posterior fossa tumours, it is important to note that these findings may not be entirely generalisable to more chronic or complex hydrocephalus syndromes seen in the wider neurosurgical population, such as low-pressure hydrocephalic states[31]; or those with altered CSF constitution, such as following subarachnoid or intraventricular haemorrhage, or central nervous system infection. In the adult literature, there is cautionary evidence that in normal pressure hydrocephalus, CBF measured using ASL is reduced in deep-seated brain regions[32], but that changes in CBF do not correlate with clinical improvement following shunting[33].

Radiotherapy has been shown to affect ASL CBF in children with posterior fossa tumours[34], and this variable – in dichotomised form due to the lack of variation in total dose – was included in the modelling analysis. It is possible that some of the increase in CBF and BuxCBF seen at the follow-up timepoint will have been accounted for by this effect, although radiotherapy was a non-significant feature of the model and diminished model performance, therefore it was discarded.

# 5. Conclusions

In children with posterior fossa tumours, CBF increases after tumour resection and at follow up scanning, and it is demonstrated for the first time that this occurs in conjunction with a decrease in the arrival time of labelled blood to several brain regions. Given the differences in BAT in this cohort, quantification of CBF using a single-PLD method alone suffers serious drawbacks; here we describe a thorough approach to CBF estimation using combined multi-TI ASL. Multivariable linear mixed-effect modelling confirms that perfusion changes are more pronounced in children presenting with symptomatic obstructive hydrocephalus requiring CSF diversion. Children with CMS had significantly higher CBF at follow-up imaging, but no differences were seen in perioperative CBF compared to those without CMS. ASL MRI shows promise as a non-invasive tool to evaluate cerebral perfusion in the setting of paediatric obstructive hydrocephalus.

# References


1 Johnston IH, Rowan JO, Harper AM, Jennett WB. Raised intracranial pressure and cerebral blood flow. I. Cisterna magna infusion in primates. *J Neurol Neurosurg Psychiatry* 1972; **35**: 285–296.

2 Johnston IH, Rowan JO. Raised intracranial pressure and cerebral blood flow. 4. Intracranial pressure gradients and regional cerebral blood flow. *J Neurol Neurosurg Psychiatry* 1974; **37**: 585–592.

3 Grubb RL, Raichle ME, Phelps ME, Ratcheson RA. Effects of increased intracranial pressure on cerebral blood volume, blood flow, and oxygen utilization in monkeys. *J Neurosurg* 1975; **43**: 385–398.

4 Jabre A, Symon L, Richards PG, Redmond S. Mean Hemispheral Cerebral Blood Flow Changes After Craniotomy. Significance and Prognostic Value. *Acta Neurochir (Wien)*

1985; **78**: 13–20.

5 Kerscher S, Schoning M, Schuhmann M. Raised ICP decreases cerebral blood flow volume in pediatric patients. In: *International Society for Paediatric Neurosurgery*. 2019.

6 Toescu S, Samarth G, Layard Horsfall H, Issitt R, Margetts B, Phipps K *et al.* Fourth ventricle tumours in children – complications and influence of surgical approach. *J Neurosurg Pediatr* 2020.

7 Yeom KW, Lober RM, Alexander A, Cheshier SH, Edwards MSB. Hydrocephalus decreases arterial spin-labeled cerebral perfusion. *Am J Neuroradiol* 2014; **35**: 1433–1439.

8 Keil VC, Hartkamp NS, Connolly DJA, Morana G, Dremmen MHG, Mutsaerts HJMM *et al.* Added value of arterial spin labeling magnetic resonance imaging in pediatric neuroradiology: pitfalls and applications. *Pediatr Radiol* 2019; **49**: 245–253.

9 Robertson PL, Muraszko KM, Holmes EJ, Sposto R, Packer RJ, Gajjar A *et al.* Incidence and severity of postoperative cerebellar mutism syndrome in children with medulloblastoma: A prospective study by the Children's Oncology Group. *J Neurosurg* 2006; **105 PEDIAT**: 444–451.

10 Gudrunardottir T, Sehested A, Juhler M, Grill J, Schmiegelow K. Cerebellar mutism: definitions, classification and grading of symptoms. *Child's Nerv Syst* 2011; **27**: 1361–1363.

11 Germanò A, Baldari S, Caruso G, Caffo M, Montemagno G, Cardia E *et al.* Reversible cerebral perfusion alterations in children with transient mutism after posterior fossa surgery. *Child's Nerv Syst* 1998; **14**: 114–119.

12 De Smet HJ, Baillieux H, Wackenier P, De Praeter M, Engelborghs S, Paquier PF *et al.* Long-Term Cognitive Deficits Following Posterior Fossa Tumor Resection: A Neuropsychological and Functional Neuroimaging Follow-Up Study. *Neuropsychology* 2009; **23**: 694–704.

13 Miller NG, Reddick WE, Kocak M, Glass JO, Lobel U, Morris B *et al.* Cerebellocerebral Diaschisis Is the Likely Mechanism of Postsurgical Posterior Fossa Syndrome in Pediatric Patients with Midline Cerebellar Tumors. *Am J Neuroradiol* 2010; **31**: 288–294.

14 Yecies D, Shpanskaya K, Jabarkheel R, Maleki M, Bruckert L, Cheshier SH *et al.* Arterial spin labeling perfusion changes of the frontal lobes in children with posterior fossa syndrome. *J Neurosurg Pediatr* 2019; : 1–7.

15 Watanabe Y, Yamasaki F, Nakamura K, Kajiwara Y, Takayasu T, Nosaka R *et al.* Evaluation of cerebellar mutism by arterial spin-labeling perfusion magnetic resonance imaging in a patient with atypical teratoid/rhabdoid tumor (AT/RT): a case report. *Childs Nerv Syst* 2012; **28**: 1257–60.

16 Alsop DC, Detre JA, Golay X, Günther M, Hendrikse J, Hernandez-Garcia L *et al.* Recommended implementation of arterial spin-labeled perfusion MRI for clinical applications: A consensus of the ISMRM perfusion study group and the European consortium for ASL in dementia. *Magn Reson Med* 2015; **73**: 102–16.

17 Dale AM, Fischl B, Sereno MI. Cortical Surface-Based Analysis. *Neuroimage* 1999; **9**: 179–194.

18 Modat M, Cash DM, Daga P, Winston GP, Duncan JS, Ourselin S. Global image registration using a symmetric block-matching approach. *J Med Imaging* 2014; **1**: 024003.

19 Buxton RB, Frank LR, Wong EC, Siewert B, Warach S, Edelman RR. A general kinetic model for quantitative perfusion imaging with arterial spin labeling. *Magn Reson Med* 1998; **40**: 383–396.

20 Hales PW, Kawadler JM, Aylett SE, Kirkham FJ, Clark CA. Arterial spin labeling characterization of cerebral perfusion during normal maturation from late childhood into

adulthood: normal ‘reference range’ values and their use in clinical studies. *J Cereb Blood Flow Metab* 2014; **34**: 776–84.

21 Jenkinson M, Bannister P, Brady M, Smith S. Improved optimization for the robust and accurate linear registration and motion correction of brain images. *Neuroimage* 2002; **17**: 825–841.

22 Team RC. R: A language and environment for statistical computing. 2017.

23 Barton K. MuMIn: Multi-Model Inference. 2020.

24 Rao VK, Haridas A, Nguyen TT, Lulla R, Wainwright MS, Goldstein JL. Symptomatic cerebral vasospasm following resection of a medulloblastoma in a child. *Neurocrit Care* 2013; **18**: 84–88.

25 Gocmen S, Acka G, Karaman K, Kahraman S. Cerebral Vasospasm after Posterior Fossa Tumor Surgery: A Case Report and Literature Review. *Pediatr Neurosurg* 2020; : 1–6.

26 Deghedy M, Pizer B, Kumar R, Mallucci C, Avula S. Basilar Artery Vasospasm as a Cause of Post-Operative Cerebellar Mutism Syndrome. *Case Rep Pediatr* 2022; **2022**: 1–5.

27 Lin CT, Riva-Cambrin JK. Management of posterior fossa tumors and hydrocephalus in children: a review. *Child's Nerv Syst* 2015; **31**: 1781–1789.

28 Borgesen SE, Gjerris F. Relationships between intracranial pressure, ventricular size, and resistance to CSF outflow. *J Neurosurg* 1987; **67**: 535–539.

29 N A, KM van B, PAJT R, EW H. Association between cerebral perfusion and paediatric postoperative cerebellar mutism syndrome after posterior fossa surgery-a systematic review. *Childs Nerv Syst* 2021. doi:10.1007/S00381-021-05225-5.

30 Hartkamp NS, Petersen ET, De Vis JB, Bokkers RPH, Hendrikse J. Mapping of cerebral perfusion territories using territorial arterial spin labeling: Techniques and clinical application. *NMR Biomed* 2013; **26**: 901–912.

31 Pang D, Altschuler E. Low-Pressure Hydrocephalic State and Viscoelastic Alterations in the Brain. *Neurosurgery* 1994; **35**: 643–656.

32 Virhammar XJ, Laurell XK, Ahlgren XA, Larsson E-M. Arterial Spin-Labeling Perfusion MR Imaging Demonstrates Regional CBF Decrease in Idiopathic Normal Pressure Hydrocephalus. doi:10.3174/ajnr.A5347.

33 Virhammar J, Ahlgren A, Cesarini KG, Laurell K, Larsson E. Cerebral Perfusion Does Not Increase after Shunt Surgery for Normal Pressure Hydrocephalus. *J Neuroimaging* 2020; : jon.12702.

34 Li MD, Forkert ND, Kundu P, Ambler C, Lober RM, Burns TC *et al.* Brain Perfusion and Diffusion Abnormalities in Children Treated for Posterior Fossa Brain Tumors. *J Pediatr* 2017; **185**: 173-180.e3.

**Table 1**. Mean post-operative cortical perfusion metrics by surgical approach. Values are mean±S.D.; p values from unpaired t-tests.

| | Midline | Hemispheric | 95% CI difference | p |
|---|---|---|---|---|
| **Age (y)** | 6.22±3.45 | 7.05±3.5 | -3.49,1.84 | 0.527 |
| **CBF (ml/100g/min)** | 44.7±11.5 | 53.4±15.5 | -23.3,5.97 | 0.212 |
| **BAT (s)** | 0.891±0.076 | 0.828±0.056 | -0.002,0.128 | 0.0576 |
| **BuxCBF (ml/100g/min)** | 109±27.8 | 135±42.3 | -70.3,18.6 | 0.209 |

**Table 2**. Multivariable linear mixed-effects modelling of CBF based on clinical, demographic and study factors. Values indicate coefficients (standard error). °, p<0.1; *, p<0.05; **, p<0.01; ***, p<0.001.

| | Mod_baseline | Mod_hcp | Mod_hcpcms |
|---|---|---|---|
| (Intercept) | 43.3(3.86)*** | 48.4(4.06)*** | 50.1(4.70)*** |
| Post-op timepoint | 6.21(2.00)** | 3.01(2.08) | 1.55(2.20) |
| Follow-up timepoint | 14.8(2.07)*** | 10.5(2.15)*** | 7.74(2.31)*** |
| Age | -0.686(0.45) | -1.17(0.53)* | -1.34(0.59)* |
| Thalamus | -5.55(1.60)*** | -5.59(1.51)*** | -5.60(1.45)*** |
| Cerebellum | -10.0(1.59)*** | -10.0(1.50)*** | -10.0(1.44)*** |
| Unsedated (vs GA) | - | 3.57(3.79) | 5.73(3.93) |
| Hydrocephalus | - | -19.4(6.04)** | -20.5(6.27)** |
| Post-op timepoint + hydrocephalus | - | 21.5(5.17)*** | 24.0(5.13)*** |
| Follow-up timepoint + hydrocephalus | - | 26.0(5.22)*** | 27.2(5.18)*** |
| CMS | - | - | -10.9(6.46)° |
| Post-op timepoint + CMS | - | - | 8.74(5.26)° |
| Follow-up timepoint + CMS | - | - | 15.6(5.28)** |
| Akaike Information Criterion | 1841.5 | 1824.7 | 1821.8 |
| Marginal $R^2$ | 0.224 | 0.290 | 0.295 |
| Conditional $R^2$ | 0.607 | 0.650 | 0.692 |